Coherent amplification in laser cooling and trapping

Tim Freegarde* and Geoff Daniell

School of Physics and Astronomy, University of Southampton, Highfield, Southampton SO17 1BJ, United Kingdom

Danny Segal

Quantum Optics and Laser Science, Imperial College, London SW7 2BZ, United Kingdom
(Received 17 September 2005; published 7 March 2006)

The optical scattering force, behind Doppler cooling and magneto-optical trapping, may be amplified without incurring additional spontaneous emission by the state-dependent coherent deflection produced by a pulsed or chirped laser field. At some cost in experimental complexity, amplified forces allow efficient cooling on narrow transitions and permit the compact deceleration of beams with reduced transverse heating, and will be of interest for molecules and atoms with open level schemes where losses following spontaneous emission would otherwise prevail. We present a general analysis of the amplification scheme, and propose an optimized, dynamic cooling scheme that allows the temperature of a sample to be reduced by around a factor of two per excited state lifetime.

Radiation pressure is the origin of many mechanisms for atomic manipulation [1]. Resulting from the transfer of a photon's momentum to the atom or molecule that absorbs it, the optical scattering force was shown as early as 1933 with the simple deflection of atomic sodium by light from a discharge lamp [2]. With the invention of the laser, the use of radiation pressure to manipulate dilute atomic samples has since become commonplace for, if the absorption strength depends upon parameters such as position, velocity or orientation, the resulting force offers a mechanism for their control. The Doppler shift provides a velocity-dependent interaction that is the key to laser cooling [3,4], while an inhomogeneous magnetic field produces a position-dependent Zeeman shift that underlies the magneto-optical trap [5]. At low temperatures, further and more subtle mechanisms appear [6–9].

Manipulation by means of the scattering force generally uses only the impulse accompanying optical absorption; a single, low power laser source suffices, and the process is insensitive to the exact strength of the radiative interaction [10,11]. Emission is left to spontaneous events, whose symmetrically distributed radiation imparts no average recoil; but a reasonable decay rate requires strongly allowed transitions, whose linewidths usually prevent cooling from reaching the recoil limit [12]. Species are limited to those with simple, closed level schemes, whereby decay repopulates the initial state to repeat the cycle. For molecules, spontaneous emission scatters population across a manifold of rovibrational states, and molecular deflection, when first demonstrated on a beam of Na_2 [13], showed a mean impulse below that of a single photon. Even atomic hyperfine structure renders a further laser necessary for optical repumping (which involves a further spontaneous decay), and practical uses of the scattering force have with few exceptions been limited to the alkali elements and isoelectronic ions.

The scattering force is confined to around a single photon impulse per excited state lifetime. This limits the capture range of magneto-optical traps [14] and defines the minimum distance needed for beam deceleration, thousands of photons being needed to counter the momentum of an atom at room temperature. Several researchers have therefore considered enhancing the scattering force by repeatedly stimulating both excitation and emission within the atomic lifetime, giving a state-dependent impulse that can greatly exceed the single photon recoil. Momentum has been transferred to atoms at three times the rate permitted by the normal spontaneous emission limited route, using counterpropagating, interleaved trains of population-inverting "π-pulses" [15] and, more robustly, an elegant demonstration of chirped adiabatic passage [16,17]. With atoms, hundreds of photon momenta have been thus transferred, while tens of impulses have been imparted to a beam of molecular sodium [18]. State-dependent π-pulse schemes have been used to increase the path separation in atomic interferometry [19]. Where the pulses overlap, this geometry creates a position-dependent force for focusing and confinement [20,21]; alternatively, combined with a velocity-selective excitation, it offers a strong cooling effect [22].

In this paper, we note that the coherent, multiphoton deflection resulting from successive interaction with alternately-propagating pulses can convert any selective excitation into a selective force, enhancing a variety of optical techniques for trapping, slowing, and cooling. Compared with the single photon recoil accompanying initial excitation, this amplifies the optical force while diluting the role of spontaneous emission. The mechanism may be regarded both as stimulated scattering and as a relation of bichromatic and moving dipole forces.

Separating the selective excitation from the impulse allows us to offer a simple analysis to guide practical applications of this phenomenon. The maximum amplification is determined by the number of pulses per excited state lifetime. As the limit set by the lifetime is approached, memory of the initial state is lost; the useful impulse ceases to grow,

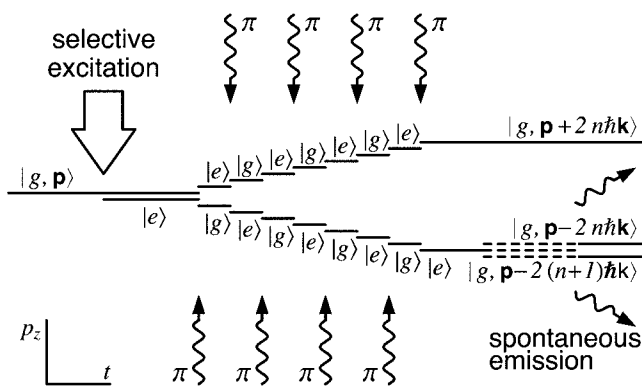*Electronic address: tim.freegarde@physics.org

FIG. 1. Scheme for amplification of the optical scattering force. Depending upon the state in which the atom is left after selective excitation, a sequence of counterpropagating π pulses either reinforces the initial impulse or accelerates the species in the opposite direction. Chirps from a frequency-modulated laser could replace the pulses shown here.

and additional pulses contribute instead to the decoherence and heating of the atomic sample. Our results allow the balance between impulse and heating to be optimized; for interferometry, for example, this allows the best combination of enclosed area and signal-to-noise ratio.

With amplified cooling, the balance between impulse and heating may be optimized for any initial distribution. We show that, by adjusting this balance as a sample is cooled, both the number of spontaneous events and the time taken may be significantly reduced from a linear to a logarithmic dependence on the typical initial momenta. By vastly increasing the ratio of the useful impulse to spontaneous decay, this may make practical the optical cooling of molecular vapors. For atomic species, amplification of the cooling force may permit the use of narrow transitions that would otherwise be too slow, allowing cooling down to the recoil limit [23].

I. AMPLIFICATION SCHEME

Whereas conventional cooling and trapping schemes ideally need only a single, low power laser for selective excitation of a closed cooling transition (as exists for Mg^+ or Be^+ ions), amplification requires a second laser system offering well controlled, relatively intense pulses tailored to provide coherent transfer between atomic states. The arrangement is shown schematically in Fig. 1.

We consider a two-level system, with ground (or principal) state g and excited state e, and assign a momentum $\mathbf{p}$, so that the overall state is written as $|\psi, \mathbf{p}\rangle$, where ψ equals g or e. The process begins with the conventional step of selectively exciting a given class of species from $|g, \mathbf{p}_0\rangle$ to $|e, \mathbf{p}_0 - \hbar\mathbf{k}\rangle$, using the usual low power laser. If this initial excitation has a velocity-dependent probability $\mathcal{P}(\mathbf{p}_0)$, then the accompanying velocity-dependent change in momentum comprises the conventional cooling process; if instead it depends upon position, then it is the basis of an optical trap. Alternatively, for interferometry, it will be the process that prepares the initial superposition of the two states.

Before the excited state decays by spontaneous emission, we use the tailored pulse laser to apply along the same axis a sequence of alternately-propagating π-pulses, each of which inverts the atomic state populations and deflects the species up or down accordingly. The key to the process is that a ground state atom suffers deflection in the direction of the pulse whereas an excited state atom recoils in a direction opposite to the incoming pulses. After n pulse pairs, and in the absence of spontaneous emission, the population is split between the states $|g, \mathbf{p}_0 + 2n\hbar\mathbf{k}\rangle$ and $|e, \mathbf{p}_0 - (2n+1)\hbar\mathbf{k}\rangle$. The momentum difference introduced by the selective excitation is thereby increased by a factor of $4n+1$. It is thus as if a second photon of momentum $4n\hbar\mathbf{k}$ had accompanied the original photon and mimicked its action.

In contrast to conventional Doppler cooling, those atoms initially left unexcited nonetheless incur a nonzero impulse. This may in many cases be useful, as it may sweep this class of atoms towards the required position or velocity whilst the selected atoms are pushed in the opposite direction. Alternatively, we may interleave pulse sequences in which the downward pulse leads so that—with the velocity selection either reversed or extinguished—a net impulse is experienced only by the selected species.

Our analysis begins by deriving the effect of a single train of pulses upon the atomic or molecular species, starting immediately after the selective excitation process; depending upon the initial state, number of pulses, and probability of decay, we obtain the mean impulse, and variance, the final state probabilities, and the likely number of intermediate decays. These results are the important parameters which determine the effectiveness of the amplification in any application, from interferometry to cooling and trapping.

We next examine the effect of the single train upon an atomic ensemble, taking as an example a generic cooling process applied to a Gaussian velocity distribution. Our analysis allows determination of the optimum parameters for the amplification scheme for a given initial velocity distribution.

Finally, we show that an appropriately tailored series of pulse trains offers a remarkable improvement in both the speed of cooling and the number of spontaneous decays likely to be incurred.

II. RESPONSE TO A SINGLE PULSE TRAIN

To determine the response of an atom to a train of pulses, we begin by considering the effect of a single pair of oppositely-traveling pulses. We start immediately before the first upward pulse (see Fig. 1) and calculate the state probabilities immediately before the next such pulse a period τ later. Depending upon the initial state of the two-level atom and whether or not spontaneous decay occurs while it is in the excited state, there are five different possibilities, shown in Table I. The probability of excited state decay within a period $\tau/2$ is taken to be $q = 1 - \exp[-(\tau/2\tau_{21})]$, where τ_{21} is the excited state lifetime. We calculate separately the impulses resulting from stimulated and spontaneous processes and characterize the momentum reached as a result of stimulated interactions through the momentum index p.

TABLE I. Interaction with a pair of oppositely-traveling pulses gives five distinct outcomes, depending upon the initial state (measured immediately before the upward pulse) and whether spontaneous decay—represented by sloping arrows—occurs while the atom is in the excited state.

			impulse	heating	probability
	$\uparrow$	$\downarrow$	Δp $(\hbar k)$	(photons)	
$\lvert g \rangle$		$\lvert g \rangle$	$+2$	0	$1-q$
$\lvert g \rangle$		$\lvert e \rangle$	0	1	$q(1-q)$
$\lvert g \rangle$		$\lvert g \rangle$	0	2	q^2
$\lvert e \rangle$		$\lvert e \rangle$	-2	0	$1-q$
$\lvert e \rangle$		$\lvert g \rangle$	-2	1	q
$n \vdots$		$n{+}1 \vdots$			

After some algebraic manipulations, given in Appendix A, we arrive at expressions describing the momentum distribution after n pulse pairs. The following expressions depend upon the probability q of excited state decay and apply to an ensemble of atoms with the same initial velocity, of which a fraction e_0 begins in the excited state. If no impulse accompanies the selective excitation, e_0 corresponds directly to the excitation probability $\mathcal{P}$.

The average momentum after n pulse pairs is given, in units of $\hbar k$, by

$$I_{n,e_0} = 2\left\{\frac{1-q}{2-q} - e_0\right\}\frac{(1-q)^{2n}-1}{(1-q)^2-1}(2-q) \qquad (1)$$

and thus when $nq \ll 1$ the relative impulse between ground and excited state atoms will be $\approx 4n$. The variance is given by

$$\Delta^2_{n,e_0} = -\frac{4}{q^2}\left\{\frac{1-q}{(2-q)^2}[q^2-3q+3] - \frac{q^2-2q+2}{2-q}e_0 + e_0^2\right\}$$
$$+ \frac{8(1-q)}{q(2-q)}n + \frac{4(1-q)^{2n}}{q^2}\{1-q-(2-q)e_0+2e_0^2\}$$
$$- \frac{4(1-q)^{4n}}{q^2}\left\{\frac{(1-q)^2}{(2-q)^2} - 2\frac{1-q}{2-q}e_0 + e_0^2\right\}. \qquad (2)$$

The average number of spontaneous decays incurred is given by

$$D_{n,e_0} = \frac{2q}{2-q}n + q^2\left(\frac{1-q}{2-q} - e_0\right)\frac{(1-q)^{2n}-1}{(1-q)^2-1}, \qquad (3)$$

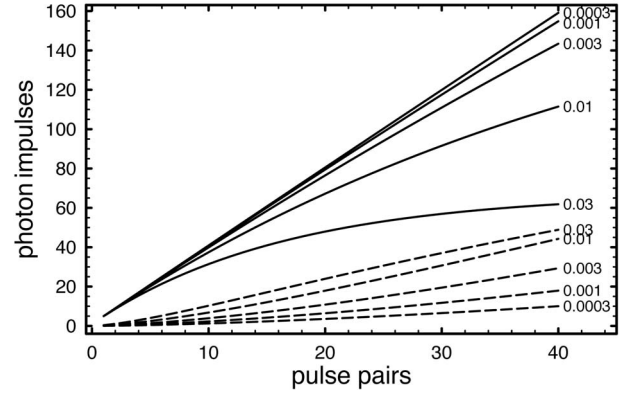and, after the pulse train, the fraction remaining excited is given by

FIG. 2. Mean relative impulse (solid lines) and heating (dashed lines) as functions of pulse train length for various decay probabilities q.

$$e_{n,e_0} = (1-q)^{2n}e_0 + \frac{1-q}{2-q}[1-(1-q)^{2n}]. \qquad (4)$$

These expressions, together with details of the processes of selective excitation and spontaneous decay, suffice to describe any implementation of the amplification scheme.

When the small additional contributions due to the initial selective impulse a and eventual spontaneous recoil α are included, and momenta are now measured with respect to those before the selective excitation, the mean impulse and heating terms become

$$I^{(T)}_{n,e_0} = e_0(a+I_{n,1}) + (1-e_0)I_{n,0} \qquad (5)$$

and

$$\Delta^{2(T)}_{n,e_0} = e_0(a+I_{n,1})^2 + (1-e_0)I^2_{n,0} - (I_{n,e_0}+ae_0)^2 + e_0\Delta^2_{n,1}$$
$$+ (1-e_0)\Delta^2_{n,0} + \alpha[e_0D_{n,1}+(1-e_0)D_{n,0}] + \alpha[e_0e_{n,1}$$
$$+ (1-e_0)e_{n,0}]. \qquad (6)$$

Figure 2 shows the relative impulse $(I^{(T)}_{n,0}-I^{(T)}_{n,1})$ and heating (standard deviation, $\Delta^{(T)}_{n,0}$) for various spontaneous decay probabilities q for pulse trains containing up to 40 pulse pairs, taking into account the initial selective impulse (with $a=-1$) and subsequent spontaneous emission ($\alpha=1/3$). As the accrued decay probability $\sim qn/2$ increases, the correlation of the atomic state with its initial value disappears and the average impulse ceases to grow, approaching a limiting value of $2/q$. Heating, in contrast, continues to increase. The dependence of the variance upon the initial state is too small to distinguish.

As the number of pulse pairs n increases, the initial impulse a becomes irrelevant, and the role of the conventional manipulation step becomes increasingly that of selective excitation.

III. APPLICATIONS

Our results may be used to determine the optimum number of pulse pairs for any implementation of the amplified scattering force. For atomic beam deceleration, for example,
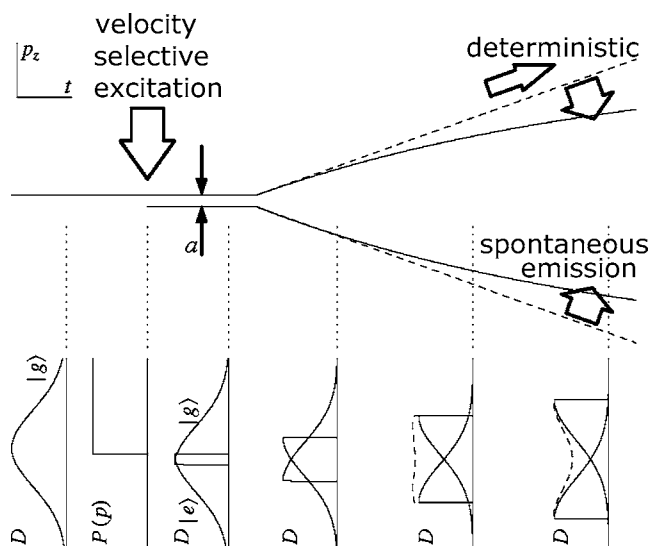
FIG. 3. Amplified cooling uses a velocity-selective excitation $\mathcal{P}(p)$ to divide the initial velocity distribution $\mathcal{D}(p)$ between the two quantum states; the small accompanying impulse a otherwise accounts for the Doppler cooling force. The optimum amplification is then determined by a combination of the best overlap of the two halves, offset by the heating due to spontaneous emission during the process.

amplification reduces the stopping distance and hence both the dimensions of the apparatus required and the transverse growth of the beam, as well as reducing the transverse heating because fewer spontaneous emissions are required for a given velocity change. The amplification is chosen to give the maximum deceleration that does not significantly heat the slowed sample. A variation of this deceleration scheme has been elegantly implemented using a bichromatic standing wave [24].

Chu and co-workers have used amplification to increase the path separation in atom interferometers [19,25–28]. Here, the sensitivity of the interferometer depends upon the phase-space area enclosed between the two interfering paths, which is increased in at least linear proportion to the amplification factor. Spontaneous emission causes some of the coherent atom flux to be lost, hence reducing the signal-to-noise ratio of the measurement. Our results may therefore be used to calculate the length of pulse train which gives the best absolute sensitivity to the measured parameter. If the interferometer encloses an area of real space, the path separation may have to be sufficient to pass around a physical object—an arrangement which so far has only been achieved using mechanical gratings [29].

IV. OPTIMUM AMPLIFIED COOLING

As an example, we consider a generic amplified cooling scheme, shown in Fig. 3. Selective excitation divides the initial velocity distribution $\mathcal{D}(p)$ between the ground and excited states with an excitation probability $\mathcal{P}(p)$, which for simplicity we take here to be a step function at $p=0$. This velocity-dependent process could be conventional Doppler
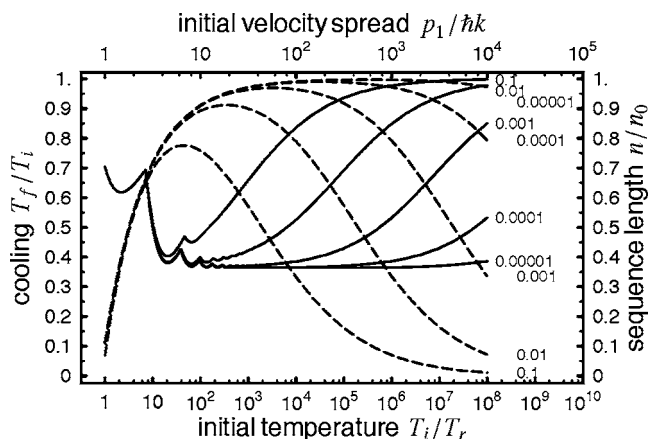

FIG. 4. Optimized cooling factor T_f/T_i (solid lines) and corresponding pulse train length n (dashed lines as fraction of decay-free optimum, $n_0=p_1/2\sqrt{\pi}$) for Gaussian velocity distributions, shown as a function of the initial temperature T_i (in units of the recoil temperature T_r) for various decay probabilities q from 0.000 01 to 0.1. The width p_1 of the initial velocity distribution is shown on the upper x axis.

cooling [3,4], interferometric cooling [30], or chirped excitation [22]. The pulse trains are then applied, and the two parts of the velocity distribution slide over each other. Finally, species in the excited state are allowed to relax to the ground state. This part of the process has been addressed by Djotyan *et al.* [31]; a related situation in which the two counterpropagating fields are present simultaneously has been extensively analysed by Kazantsev *et al.* [32].

In the absence of spontaneous emission, any magnitude of amplified impulse may be chosen, and the optimum is simply that which gives the best overlap of the two fractions. Spontaneous emission may cause this desired relative impulse to exceed the maximum $(2\hbar k/q)$ possible, or result in significant heating of the sample; the optimum pulse train will then be somewhat shorter.

Our results allow calculation of the optimum pulse length and its cooling effect, shown in Fig. 4 for velocity distributions that are initially Gaussian. Details of the calculation are given in Appendix C. As we shall see, displaying these parameters as a function of initial temperature will allow us to identify a particular cooling strategy. The curves show the optimized cooling factor—the ratio of final to initial temperatures, T_f/T_i—and the corresponding number of pulse pairs required, n, as a multiple of the optimum number n_0 when $q=0$. It is apparent that a substantial reduction in temperature can be achieved even within an excited state lifetime by a single pulse train, whose optimum length depends upon the initial temperature of the atomic sample. n is taken to be an integer when calculating T_f/T_i, but for clarity is allowed to vary smoothly in the presentation of n/n_0.

Consider first the solid lines showing T_f/T_i in Fig. 4. For low initial temperatures, the final spontaneous recoil is significant, and limits the cooling effect that may be achieved. T_f/T_i therefore falls with increasing initial velocity spread, irrespective of the decay probability q, and rapidly reaches a limiting value of around 0.36, described below. Some undulations are apparent simply because the optimum number of

pulse pairs must jump abruptly between integer values, for $T_i/T_r < \sim 8$, for example, the best integer value of n is 0, and the process is identical to conventional Doppler cooling. For low values of q, T_f/T_i then remains quite level for a wide range of initial temperatures, and the optimum cooling can always be achieved without a significant probability of decay.

The lower limit to T_f/T_i corresponds simply to the optimum overlap of the two halves of the velocity distribution. In the absence of significant spontaneous emission, the two halves of an initially rectangular distribution could be overlapped perfectly, halving its width and reducing its variance and temperature by a factor of four. For a distribution that is initially Gaussian, the overlap is less perfect, and the optimum overlap gives a reduction in variance of a factor of $(1-2/\pi) \approx 0.36$.

As the range of initial velocities or decay rate q is increased, this optimum overlap demands more pulses than can be applied without decay limiting their effectiveness, and the temperature can no longer be reduced by the same factor. This limit is reached first for the broadest velocity distributions, but affects increasingly lower initial temperatures as the decay probability q is increased. Ultimately, the best that we can do is to apply a constant impulse, depending upon the decay probability q, that has an ever less obvious effect upon the broader velocity distributions—although it is of course greater than that offered by the unamplified cooling scheme alone.

If we now consider the variation in the sequence length n/n_0 as a function of the initial temperature—shown by the dashed curves in Fig. 4—we see that for low values of q the sequence length approaches unity as soon as the spontaneous recoil can be neglected. This initial behavior is also in part an artifact associated with the presentation, for clarity, of a smoothly-varying function that corresponds to noninteger values of n and n_0. Provided that the decay probability q is sufficiently small, the pulse length may then maintain its ideal value for increasingly broad velocity distributions, until eventually decay begins to limit the useful impulse, and the optimum length falls below the ideal.

These results suggest a cooling strategy that, at a modest expense in experimental complexity, offers a number of significant improvements over conventional Doppler cooling. Beginning with a broad distribution of velocities, a series of cycles of excitation, amplification, and relaxation is applied, each optimized to the pertaining temperature of the sample. Initially, a large impulse is imparted, incurring a relatively large variance which is nonetheless insignificant compared with that of the sample. The process is then repeated on the now somewhat narrower distribution, which requires a shorter pulse train and hence results in rather less heating. This pattern can be continued, adapting the pulse length at each stage to the expected initial temperature, reaching the limit of unamplified conventional cooling. This dynamic variation of the interaction may be compared with that of Kasevich and Chu and Davidson *et al.* [33,34].

Whereas conventional cooling would impart less than a photon impulse per excited state lifetime, and hence require a time proportional to the width of the initial velocity distribution, the duration of the dynamically-adjusted, amplified arrangement depends upon its logarithm. To cool a rectangular distribution of velocities of width $10\,000\hbar k$ to its recoil limit, for example, would conventionally take 10 000 lifetimes; with dynamically adjusted amplification, this could instead be achieved in $\log_2(10\,000) \approx 13$. Far fewer spontaneous photons then contribute to transverse heating.

Amplification allows effective cooling to be achieved even on narrow transitions whose lifetimes are too long for conventional cooling schemes [35], opening up a regime in which the limiting temperature is no longer determined by the photon scattering rate $\hbar\Gamma/2 \equiv \hbar/2T$. With amplification, Doppler cooling directly to the recoil limit should be possible. It could then be applied to very long-lived Raman transitions, with the velocity-selective excitation following the scheme of Kasevich *et al.* [25,36] and relaxation induced actively by pumping to a short-lived excited state.

Finally, the number of times the species have to be repumped after relaxation is reduced to a level that might even be achieved efficiently with open-level atoms and molecules. To retain half the sample after 10 000 repumping cycles requires an individual efficiency of 99.99%; for only 15 cycles, this is reduced to 95%.

V. CONCLUSION

The optical scattering forces, used for Doppler cooling, beam deceleration, atom interferometry, and magneto-optical trapping, may be amplified by using the state-dependent interaction with counterpropagating interleaved trains of population-inverting laser pulses. This coherent amplification increases the useful impulse per excited state lifetime, permitting the use of narrow atomic transitions and reducing the distance required to decelerate fast or heavy species. By increasing the impulse per spontaneous event, amplification reduces both transverse heating and the number of repumping cycles required, rendering accessible species such as molecules with open level schemes.

We have presented here a general analysis that allows the performance of coherent amplification to be evaluated and optimized for a range of applications. For atom interferometry, our results allow the optimum pulse sequence to be determined, balancing the interferometer area against atom flux to give the best overall sensitivity. Enhancements to Doppler cooling allow the temperature of a sample to be reduced by a factor approaching four per excited state lifetime. This suggests a dynamically adjusted cooling scheme in which the time taken, and the number of spontaneous events suffered, depends logarithmically rather than linearly upon the number of photon impulses required.

Although we have for simplicity cast our scheme in terms of population-inverting π-pulses, practical implementations would most likely use more robust, chirped interactions, such as Raman adiabatic passage [37–42]. As such arrangements are also capable of the initial selective excitation itself, for both velocity-selection [30] and interferometry [27,43], such schemes may be regarded as specific manifestations of the mechanical manipulations possible on a momentum-state quantum computer [44].

APPENDIX A: RESPONSE TO A SINGLE PULSE-TRAIN

Our analysis of amplified cooling is approached in three stages. First, we derive the effect of a single train of pulses upon the species, starting immediately after selective excitation; depending upon the initial state, number of pulses, and probability of decay, we obtain the mean impulse and variance, the final state probabilities and the likely number of intermediate decays. Then, using these results, we analyze the overall effect upon an initial velocity distribution. Finally, we establish, in terms of the velocity-selective excitation characteristics, the optimum length of the pulse train and its effect upon the distribution of species velocities.

To determine the response of an atom to a train of pulses, we begin by considering the effect of a single pair of oppositely traveling pulses, starting immediately before that travelling in the positive direction, and calculate the state probabilities immediately before the next in that direction a period τ later. Depending upon the initial state of the two-level atom and whether or not spontaneous decay occurs while it is in the excited state, there are five different possibilities, shown in Table I. The probability of excited state decay within a period $\tau/2$ is taken to be $q=1-\exp[-(\tau/2\tau_{21})]$, where τ_{21} is the excited state lifetime. We calculate separately the impulses resulting from stimulated and spontaneous processes and characterize the momentum reached through stimulated interactions through the momentum index p.

If the $(n+1)$-th measurement finds the atom in the ground state with a momentum of $p\hbar k$, then at the time of the nth measurement it could have been in the ground state with two momentum units less (no spontaneous decays), or the ground state with the same momentum (two spontaneous decays), or the excited state with two momentum units more (one spontaneous decay). If $P_n(s,p)$ indicates the probability of being in state $s=g,e$ and having a momentum of $p\hbar k$ at the time of the nth measurement then, taking into account the probabilities of the various events, we may write

$$P_{n+1}(g,p) = (1-q)P_n(g,p-2) + q^2 P_n(g,p) + q P_n(e,p+2),$$
(A1)

$$P_{n+1}(e,p) = q(1-q)P_n(q,p) + (1-q)P_n(e,p+2).$$
(A2)

These recursion relations allow the state probability distribution to be determined in terms of the initial conditions. We define

$$g_n = \sum_{p=-\infty}^{\infty} P_n(g,p) \text{ and } e_n = \sum_{p=-\infty}^{\infty} P_n(e,p)$$
(A3)

and note that

$$\sum_{p=-\infty}^{\infty} P_n(g,p \pm 2) = \sum_{p=-\infty}^{\infty} P_n(g,p)$$
(A4)

and similarly for the excited state, so that

$$g_{n+1} = (1-q+q^2)g_n + qe_n,$$
(A5)

$$e_{n+1} = q(1-q)g_n + (1-q)e_n.$$
(A6)

Working is simplified by writing $g_n = n_n^+ + n_n^-$ and $e_n = (1-q)n_n^+ - n_n^-$, so that

$$\begin{pmatrix} n_{n+1}^+ \\ n_{n+1}^- \end{pmatrix} = \begin{bmatrix} 1 & 0 \\ 0 & (1-q)^2 \end{bmatrix} \begin{pmatrix} n_n^+ \\ n_n^- \end{pmatrix}.$$
(A7)

The sum of the ground and excited state populations, to which n_n^+ corresponds, is therefore happily constant, while the second term gives $n_n^- = (1-q)^{2n}n_0^-$ and hence an excited state probability

$$e_n = (1-q)^{2n}e_0 + \frac{1-q}{2-q}[1-(1-q)^{2n}].$$
(A8)

To determine the average momentum, we further define

$$G_n = \sum_{p=-\infty}^{\infty} pP_n(g,p) \text{ and } E_n = \sum_{p=-\infty}^{\infty} pP_n(e,p)$$
(A9)

which represent the ground and excited state contributions to the average momentum, and observe that

$$\sum_{p=-\infty}^{\infty} pP_n(g,p \pm 2) = \sum_{p=-\infty}^{\infty} (p \pm 2)P_n(g,p \pm 2) \mp 2P_n(g,p \pm 2)$$

$$= G_n \mp 2g_n.$$
(A10)

Once again, the recursion matrix is diagonalized by considering the combinations $G_n = N_n^+ + N_n^-$ and $E_n = (1-q)N_n^+ - N_n^-$,

$$\begin{pmatrix} N_{n+1}^+ \\ N_{n+1}^- \end{pmatrix} = \begin{bmatrix} 1 & 0 \\ 0 & (1-q)^2 \end{bmatrix} \begin{pmatrix} N_n^+ \\ N_n^- \end{pmatrix} + \begin{bmatrix} 0 & 1 \\ (1-q)^2 & 0 \end{bmatrix} \begin{pmatrix} n_n^+ \\ n_n^- \end{pmatrix}.$$
(A11)

The average momentum of the ensemble is hence given by

$$I_{n,e_0} = G_n + E_n = (2-q)N_n^+$$

$$= 2\left\{\frac{1-q}{2-q} - e_0\right\} \frac{(1-q)^{2n}-1}{(1-q)^2-1}(2-q).$$
(A12)

Derivation of the mean-squared momentum follows the same route. We define

$$\Gamma_n = \sum_{p=-\infty}^{\infty} p^2 P_n(g,p) \text{ and } \mathcal{E}_n = \sum_{p=-\infty}^{\infty} p^2 P_n(e,p)$$
(A13)

so that the mean-squared momentum is given by $\Delta_n^2 = \Gamma_n + \mathcal{E}_n - I_n^2$. Since $p^2 \equiv (p \pm 2)^2 \mp 4(P \pm 2) + 4$, we have

$$\sum_{p=-\infty}^{\infty} p^2 P_n(g,p \pm 2) = \sum_{p=-\infty}^{\infty} (p \pm 2)^2 P_n(g,p \pm 2)$$

$$\mp 4(p \pm 2)P_n(g,p \pm 2) + 4P_n(g,p)$$

$$= \Gamma_n \mp 4G_n + 4g_n.$$
(A14)

Diagonalization requires the combinations $\Gamma_n = H_n^+ + H_n^-$ and $\mathcal{E}_n = (1-q)H_n^+ - H_n^-$, giving

$$\begin{pmatrix} H_{n+1}^+ \\ H_{n+1}^- \end{pmatrix} = \begin{bmatrix} 1 & 0 \\ 0 & (1-q)^2 \end{bmatrix} \begin{pmatrix} H_n^+ \\ H_n^- \end{pmatrix} + 4 \begin{bmatrix} 0 & 1 \\ (1-q)^2 & 0 \end{bmatrix} \begin{pmatrix} N_n^+ \\ N_n^- \end{pmatrix}$$

$$+ \frac{4}{2-q} \begin{bmatrix} 2(1-q) & -q \\ (1-q)^2 q & 2(1-q)^2 \end{bmatrix} \begin{pmatrix} n_n^+ \\ n_n^- \end{pmatrix} \quad \text{(A15)}$$

and hence

$$\Delta_{n,e_0}^2 = \Delta_0^2 + I_0^2 - I_n^2 + \frac{8(1-q)}{q(2-q)}n + 4 \left\{ \frac{2(1-q)^2}{q^2(2-q)^2} + \frac{1-q}{(2-q)^2} \right.$$

$$\left. - \frac{e_0}{2-q} - \frac{N_0}{q} \right\} [(1-q)^{2n} - 1]. \quad \text{(A16)}$$

Inserting I_n, taking $I_0 = N_0^- = 0$ and writing $n_0^- = (1-q)/(2-q) - e_0$ hence gives

$$\Delta_{n,e_0}^2 = \Delta_0^2 - \frac{4}{q^2} \left\{ \frac{1-q}{(2-q)^2}[q^2 - 3q + 3] - \frac{q^2 - 2q + 2}{2-q}e_0 + e_0^2 \right\}$$

$$+ \frac{8(1-q)}{q(2-q)}n + \frac{4(1-q)^{2n}}{q^2} \{1 - q - (2-q)e_0 + 2e_0^2\}$$

$$- \frac{4(1-q)^{4n}}{q^2} \left\{ \frac{(1-q)^2}{(2-q)^2} - 2\frac{1-q}{2-q}e_0 + e_0^2 \right\}. \quad \text{(A17)}$$

The probability of spontaneous emission in the period ending with the $(n+1)$-th measurement is the sum of the probabilities for the two half-periods,

$$d_{n,e_0} = q(1 - e_{n-1}) + q[e_{n-1} + q(1 - e_{n-1})] = q(1+q) - q^2 e_{n-1}. \quad \text{(A18)}$$

Taking the previously derived result for e_n and summing over all periods gives an accrued number of spontaneous decays

$$D_{n,e_0} = \sum_{m=1}^{n} q(1+q) - q^2 e_{m-1}$$

$$= \frac{2q}{2-q}n + q^2 \left(\frac{1-q}{2-q} - e_0 \right) \frac{(1-q)^{2n} - 1}{(1-q)^2 - 1}. \quad \text{(A19)}$$

Each complete cycle of an amplified process incurs two further contributions to the impulse. The first—which accounts for the conventional scattering force, and which we assign a magnitude a—accompanies the initial selective excitation; this is correlated with the subsequent amplified impulse, and must therefore be taken into account explicitly. The second results from the D_{n,e_0} spontaneous emissions during the pulse train and the e_{n,e_0} emissions during subsequent relaxation and, as the directions of the spontaneous recoils are uncorrelated to other impulses, these contributions to the variance may be added directly. We take the spontaneous photon's contribution to the variance to be α, where for isotropic emission $\alpha = 1/3$ for the x component of the momentum distribution and $\alpha = 1$ when the true three-dimensional temperature is calculated. Including these terms results in a total impulse of

$$I_{n,e_0}^{(T)} = e_0(a + I_{n,1}) + (1 - e_0)I_{n,0} \quad \text{(A20)}$$

and a variance given by

$$\Delta_{n,e_0}^{2(T)} = e_0(a + I_{n,1})^2 + (1 - e_0)I_{n,0}^2 - (I_{n,e_0} + ae_0)^2 + e_0\Delta_{n,1}^2$$

$$+ (1 - e_0)\Delta_{n,0}^2 + \alpha[e_0 D_{n,1} + (1 - e_0)D_{n,0}] + \alpha[e_0 e_{n,1}$$

$$+ (1 - e_0)e_{n,0}]. \quad \text{(A21)}$$

We note that some aspects of this analysis have been covered in a full quantum-mechanical density-matrix treatment [45].

APPENDIX B: EFFECT UPON MOMENTUM DISTRIBUTION

We now consider the effect of a pulse train upon a sample of species with a distribution of velocities, which initially undergo velocity-selective excitation with a momentum-dependent probability $\mathcal{P}(p)$, accompanied by the recoil a of the conventional scattering force. The mean momentum following the pulse train of Appendix A will be given, extending Eq. (A20), by

$$\langle p' \rangle = \langle \mathcal{P}(p)[p + I_{n,1} + a] + [1 - \mathcal{P}(p)][p + I_{n,0}] \rangle$$

$$= \langle p \rangle + I_{n,0} + \langle \mathcal{P}(p) \rangle [a + I_{n,1} - I_{n,0}], \quad \text{(B1)}$$

where I_{n,e_0} is the mean impulse for an initial excitation probability e_0 and the bra-ket notation indicates the average over the initial velocity distribution, which is not explicitly defined. Similarly, if all species with the same initial state were to receive the same impulse, the mean squared momentum of the final distribution would be given by

$$\langle p'^2 \rangle = \langle \mathcal{P}(p)[p + I_{n,1} + a]^2 + [1 - \mathcal{P}(p)][p + I_{n,0}]^2 \rangle$$

$$= \langle p^2 \rangle + I_{n,0}^2 + 2\langle p \rangle I_{n,0} + \langle \mathcal{P}(p) \rangle [a^2 + I_{n,1}^2$$

$$- I_{n,0}^2 + 2aI_{n,1}] + 2\langle p\mathcal{P}(p) \rangle [a + I_{n,1} - I_{n,0}]. \quad \text{(B2)}$$

Combining these expressions leads, with a little rearrangement, to the variance of the final momentum distribution,

$$\langle p'^2 \rangle - \langle p' \rangle^2 = \langle p^2 \rangle - \langle p \rangle^2 + \langle \mathcal{P}(p) \rangle [1 - \langle \mathcal{P}(p) \rangle][a + I_{n,1}$$

$$- I_{n,0}]^2 + 2\langle (p - \langle p \rangle)\mathcal{P}(p) \rangle [a + I_{n,1} - I_{n,0}], \quad \text{(B3)}$$

where the terms correspond to the variance of the initial distribution, the separation according to quantum state following selective excitation, and cooling due to a correlation between the excitation probability and initial velocity.

To this final variance, we should now add heating contributions from the spread about the mean impulse, Δ_n^2, and the recoils accompanying spontaneous emission during and after the pulse train. If α is the contribution to the variance for each spontaneous event, then the variance will be given by

$$\langle p'^2 \rangle - \langle p' \rangle^2 = \langle p^2 \rangle - \langle p \rangle^2 + \langle \mathcal{P}(p) \rangle [1 - \langle \mathcal{P}(p) \rangle][a + I_{n,1}$$

$$- I_{n,0}]^2 + 2\langle (p - \langle p \rangle)\mathcal{P}(p) \rangle [a + I_{n,1} - I_{n,0}]$$

$$+ \Delta_{n,0}^2 + \langle \mathcal{P}(p) \rangle [\Delta_{n,1}^2 - \Delta_{n,0}^2] + \alpha\{D_{n,0} + \langle \mathcal{P}(p) \rangle$$

$$\times [D_{n,1} - D_{n,0}]\} + \alpha\{e_{n,0} + \langle \mathcal{P}(p) \rangle [e_{n,1} - e_{n,0}]\}. \quad \text{(B4)}$$

I_{n,e_0}, Δ^2_{n,e_0}, D_{n,e_0}, and e_{n,e_0} are the mean impulse, impulse variance, mean number of spontaneous decays, and final excitation probability for the pulse train, given in Appendix A; a and α are the recoils accompanying the initial selective excitation and subsequent spontaneous emission; $\langle p^2 \rangle - \langle p \rangle^2$ corresponds to the initial temperature of the sample. The mean probability of selective excitation, $\langle \mathcal{P}(p) \rangle$ and the correlation $\langle (p - \langle p \rangle)\mathcal{P}(p) \rangle$ depend upon the initial velocity distribution and excitation selectivity.

APPENDIX C: OPTIMUM COOLING STRATEGY

We may now determine the optimum length of pulse train for a given initial velocity distribution by setting to zero the derivative of Eq. (B4) with respect to n. In the limit $q \to 0$, we obtain

$$4n = a + \frac{\langle (p - \langle p \rangle)\mathcal{P}(p) \rangle}{\langle \mathcal{P}(p) \rangle [1 - \langle \mathcal{P}(p) \rangle]} \qquad (C1)$$

which, if the average probability of selective excitation $\langle \mathcal{P}(p) \rangle = \frac{1}{2}$, gives

$$4n = a + 4\langle (p - \langle p \rangle)\mathcal{P}(p) \rangle \qquad (C2)$$

and hence a variance of

$$\langle p'^2 \rangle - \langle p' \rangle^2 = \langle p^2 \rangle - \langle p \rangle^2 - 4\langle (p - \langle p \rangle)\mathcal{P}(p) \rangle + \frac{\alpha}{2}. \qquad (C3)$$

For an initially Gaussian, Maxwellian velocity distribution of temperature T_i,

$$\mathcal{D}(p) = \frac{1}{p_1 \sqrt{\pi}} \exp\left[-\left(\frac{p}{p_1} \right)^2 \right], \qquad (C4)$$

where $p_1^2 = T_i / T_r$ in terms of the recoil temperature $T_r = \hbar^2 k^2 / 2m k_B$, we find that $\langle p^2 \rangle = p_1^2 / 2$. Taking the selective excitation probability to be a step function

$$\mathcal{P}(p) = \begin{cases} 1 & p \geq 0 \\ 0 & p < 0 \end{cases}, \qquad (C5)$$

we obtain a final variance of

$$\langle p'^2 \rangle - \langle p' \rangle^2 = \frac{p_1^2}{2}\left(1 - \frac{2}{\pi} \right) + \frac{\alpha}{2}. \qquad (C6)$$

Although the velocity distribution will no longer be Gaussian, the variance remains a measure of its average kinetic energy and will indeed represent the temperature obtained if the sample is allowed to come to thermal equilibrium. With this caveat, we may may hence consider the temperature of the distribution to have been reduced, if the term $\alpha/2$ may be neglected, by a factor of $\beta = (1 - 2/\pi) \approx 0.36$.

If the impulse accompanying the initial selective excitation may be neglected in Eq. (C2), the optimum number of pulses becomes approximately

$$n_0 = \langle (p - \langle p \rangle)\mathcal{P}(p) \rangle = p_1 / 2\sqrt{\pi}. \qquad (C7)$$

After relaxation of excited state atoms to the ground state through spontaneous decay, the sample may once again be cooled with a further newly-optimized pulse train. Strictly, the optimum factor β depends upon the shape of the velocity distribution, whose variance becomes increasingly dominated by the small number of atoms with large velocities remaining in the tail of the initial Gaussian. For practical purposes, however, similar values of β will generally be required. After m cycles of selective excitation-amplification-relaxation, the final temperature will be given roughly by

$$T_m = \beta^m T_0. \qquad (C8)$$

As each cycle occurs within the same spontaneous lifetime, the time taken to achieve a given temperature hence depends logarithmically, rather than linearly, upon the number of photon impulses required. Numerical results for cases in which the decay probability q may not be neglected are given in Fig. 4.

[1] S. Chu, Science **253**, 861 (1991).

[2] R. Frisch, Z. Phys. **86**, 42 (1933).

[3] T. W. Hänsch and A. L. Schawlow, Opt. Commun. **13**, 68 (1975).

[4] D. J. Wineland and H. Dehmelt, Bull. Am. Phys. Soc. **20**, 637 (1975).

[5] E. L. Raab, M. Prentiss, A. Cable, S. Chu, and D. E. Pritchard, Phys. Rev. Lett. **59**, 2631 (1987).

[6] A. Aspect, J. Dalibard, A. Heidmann, C. Salomon, and C. Cohen-Tannoudji, Phys. Rev. Lett. **57**, 1688 (1986).

[7] A. Aspect, E. Arimondo, R. Kaiser, N. Vansteenkiste, and C. Cohen-Tannoudji, Phys. Rev. Lett. **61**, 826 (1988).

[8] J. Dalibard and C. Cohen-Tannoudji, J. Opt. Soc. Am. B **6**, 2023 (1989).

[9] P. J. Ungar, D. S. Weiss, E. Riis, and S. Chu, J. Opt. Soc. Am. B **6**, 2058 (1989).

[10] D. J. Wineland, R. E. Drullinger, and F. L. Walls, Phys. Rev. Lett. **40**, 1639 (1978).

[11] W. Neuhauser, M. Hohenstatt, P. Toschek, and H. Dehmelt, Phys. Rev. Lett. **41**, 233 (1978).

[12] H. J. Metcalf and P. van der Straten, J. Opt. Soc. Am. B **20**, 887 (2003).

[13] A. Herrmann, S. Leutwyler, L. Wöste, and E. Schumacher, Chem. Phys. Lett. **62**, 444 (1979).

[14] H. Metcalf, J. Opt. Soc. Am. B **6**, 2206 (1989).

[15] B. Nölle, H. Nölle, J. Schmand, and H. J. Andrä, Europhys. Lett. **33**, 261 (1996).

[16] M. Cashen, O. Rivoire, L. Yatsenko, and H. Metcalf, J. Opt. B: Quantum Semiclassical Opt. **4**, 75 (2002).

[17] M. Cashen and H. Metcalf, J. Opt. Soc. Am. B **20**, 915 (2003).

[18] V. S. Voitsekhovich, M. V. Danileiko, A. M. Negriiko, and V. I. Romanenko, JETP Lett. **59**, 408 (1994).

[19] D. S. Weiss, B. C. Young, and S. Chu, Appl. Phys. B **59**, 217 (1994).

[20] T. G. M. Freegarde, J. Walz, and T. W. Hänsch, Opt. Commun. **117**, 262 (1995).

[21] A. Goepfert, I. Bloch, D. Haubrich, F. Lison, R. Schütze, R. Wynands, and D. Meschede, Phys. Rev. A **56**, R3354 (1997).

[22] J. S. Bakos, G. P. Djotyan, G. Demeter, and Z. Sörlei, Phys. Rev. A **53**, 2885 (1996).

[23] T. Binnewies, G. Wilpers, U. Sterr, F. Riehle, J. Helmcke, T. E. Mehlstäubler, E. M. Rasel, and W. Ertmer, Phys. Rev. Lett. **87**, 123002 (2001).

[24] J. Söding, R. Grimm, Y. B. Ovchinnikov, P. Bouyer, and C. Salomon, Phys. Rev. Lett. **78**, 1420 (1997).

[25] M. Kasevich and S. Chu, Appl. Phys. B **54**, 321 (1992).

[26] D. S. Weiss, B. C. Young, and S. Chu, Phys. Rev. Lett. **70**, 2706 (1993).

[27] M. Weitz, B. C. Young, and S. Chu, Phys. Rev. Lett. **73**, 2563 (1994).

[28] A. Peters, K. Y. Chung, B. Young, J. Hensley, and S. Chu, Philos. Trans. R. Soc. London, Ser. A **355**, 2223 (1997).

[29] C. R. Ekstrom, J. Schmiedmayer, M. S. Chapman, T. D. Hammond, and D. E. Pritchard, Phys. Rev. A **51**, 3883 (1995).

[30] M. Weitz and T. W. Hänsch, Europhys. Lett. **49**, 302 (2000).

[31] G. P. Djotyan, J. S. Bakos, G. Demeter, and Z. Sörlei, J. Opt. Soc. Am. B **13**, 1697 (1996).

[32] A. P. Kazantsev, G. I. Surdutovich, D. O. Chudesnikov, and V. P. Yakovlev, J. Opt. Soc. Am. B **6**, 2130 (1989).

[33] M. Kasevich and S. Chu, Phys. Rev. Lett. **69**, 1741 (1992).

[34] N. Davidson, H.-J. Lee, M. Kasevich, and S. Chu, Phys. Rev. Lett. **72**, 3158 (1994).

[35] C. S. Adams, S. G. Cox, E. Riis, and A. S. Arnold, J. Phys. B **36**, 1933 (2003).

[36] M. Kasevich, D. S. Weiss, E. Riis, K. Moler, S. Kasapi, and S. Chu, Phys. Rev. Lett. **66**, 2297 (1991).

[37] G. P. Djotyan, J. S. Bakos, G. Demeter, P. N. Ignácz, M. A. Kedves, Z. Sörlei, J. Szigeti, and Z. L. Tóth, Phys. Rev. A **68**, 053409 (2003).

[38] L. S. Goldner, C. Gerz, R. J. C. Spreeuw, S. L. Rolston, C. I. Westbrook, W. D. Phillips, P. Marte, and P. Zoller, Quantum Opt. **6**, 387 (1994).

[39] L. S. Goldner, C. Gerz, R. J. C. Spreeuw, S. L. Rolston, C. I. Westbrook, W. D. Phillips, P. Marte, and P. Zoller, Phys. Rev. Lett. **72**, 997 (1994).

[40] P. Marte, P. Zoller, and J. L. Hall, Phys. Rev. A **44**, R4118 (1991).

[41] R. Grimm, J. Söding, and Y. B. Ovchinnikov, Opt. Lett. **19**, 658 (1994).

[42] S. Gupta, A. E. Leanhardt, A. D. Cronin, and D. E. Pritchard, C.R. Acad. Sci., Ser. IIc: Chim **2**, 479 (2001).

[43] M. Weitz, B. C. Young, and S. Chu, Phys. Rev. A **50**, 2438 (1994).

[44] T. Freegarde and D. Segal, Phys. Rev. Lett. **91**, 037904 (2003).

[45] G. Demeter, G. P. Djotyan, and J. S. Bakos, J. Opt. Soc. Am. B **15**, 16 (1998).